International Journal of Thermophysics, Vol. 19, No. 1, 1998

Molar Heat Capacity at Constant Volume of *n*-Butane at Temperatures from 141 to 342 K and at Pressures to 33 MPa

J. W. Magee[1, 2] and T. O. D. Lüddecke[1, 3]

Received September 16, 1997

Molar heat capacities at constant volume (C_v) for normal butane are presented. Temperatures ranged from 141 to 342 K for pressures up to 33 MPa. Measurements were conducted on liquid in equilibrium with its vapor and on compressed liquid samples. The high purity of the samples was verified by chemical analysis. For the samples, calorimetric results were obtained for two-phase [$C_v^{(2)}$], saturated liquid (C_σ or C'_x), and single-phase (C_v) molar heat capacities. The principal sources of uncertainty are the temperature rise measurement and the change-of-volume work adjustment. The expanded uncertainty (i.e., a coverage factor $k = 2$ and thus a two-standard deviation estimate) for values of C_v is estimated to be 0.7%, for $C_v^{(2)}$ it is 0.5%, and for C_σ it is 0.7%.

KEY WORDS: butane; compressed liquid; density; heat capacity; isochoric; saturated liquid.

1. INTRODUCTION

One of the long-range objectives of thermophysical property research at the National Institute of Standards and Technology (NIST) is the development of accurate predictive methods for calculating the properties of gaseous and liquid mixtures. These models play a key role in process equipment design, in metering applications, and in the design and operation of transportation systems such as pipelines. The ongoing development and testing of these

[1] Physical and Chemical Properties Division, National Institute of Standards and Technology, 325 Broadway, Boulder, Colorado 80303-3328, U.S.A.

[2] To whom correspondence should be addressed.

[3] Guest researcher from the Institute for Thermodynamics, University of Hannover, Hannover, Germany.

0195-928X/00/0700-0129$18.00/0

models rely heavily on benchmark experimental measurements. These measurements are conducted on selected pure components and their mixtures to provide a database which is representative of broad classes of fluid types.

Normal butane (n-C_4H_{10}) is a key component of natural gas. Knowledge of the thermophysical properties for the pure components and their mixtures is vital to the development of predictive models for natural gas mixtures. Previously, our group has measured heat capacities for methane [1], ethane [2], propane [3], (methane + ethane) mixtures [4], and (carbon dioxide + ethane) mixtures [5]. The thermodynamic properties and equation of state for n-butane have been studied by Haynes and Goodwin [6] and Sychev et al. [7]. As pointed out in both references, no published isochoric heat capacity data were available at the time of their work. Together with published density data, heat capacity measurements will provide a database for developing improved equations of state and testing predictive models for n-butane and mixtures containing this substance.

2. MEASUREMENTS

2.1. Procedure

The heat-capacity measurements in this study were performed in the calorimeter described by Goodwin [8] and Magee [9]. Briefly, in this method, a sample of well-established mass (or number of moles; n) is confined to a bomb of approximately 73 cm^3 volume; as shown in Ref. 9, the exact volume varies with temperature and pressure. When a precisely measured electrical energy (Q) is applied, the resulting temperature rise ($\Delta T = T_2 - T_1$) is measured. When both the energy (Q_0) required to heat the empty bomb and the pV work (W_{pV}) are subtracted from the total, the heat capacity is

$$C_v = \left(\frac{\partial U}{\partial T}\right)_v \cong \frac{Q - Q_0 - W_{pv}}{n\,\Delta T} \tag{1}$$

For this study, a sample was charged to the bomb, then the charge valve was sealed. The bomb and its contents were then cooled to the starting temperature. Then, measurements were begun and continued in the single-phase region until either the upper temperature (about 345 K) or the pressure (35 MPa) was obtained. At the completion of a run, some of the sample was discharged to obtain the next filling density. Difference weighings of a discharge cylinder gave the sample masses. A series of such

runs at different densities (ρ) completes the $C_v(\rho, T)$ surface for the substance under study.

Adjustments must be applied to the raw data for the energy required to heat the empty calorimeter from the initial (T_1) to the final (T_2) temperature. This is accomplished using the results of previous experiments done with a thoroughly evacuated bomb. These results were fitted to a 12-parameter polynomial $Q_0(T)$ given previously [9].

Additionally, an adjustment for pV work done by the fluid on the thin-walled bomb as the pressure rises from p_1 to p_2 is applied for each point. Corrections for pV work on the bomb were calculated by an equation discussed in a previous publication [10] from this laboratory:

$$W_{pV} = \left(T_2 \left(\frac{\partial p}{\partial T} \right)_{V_2} - \frac{\Delta p}{2} \right) \Delta V \tag{2}$$

where $\Delta p = p_2 - p_1$ is the pressure rise and $\Delta V = V_2 - V_1$ is the change of volume. The derivative has been calculated with a published equation of state for *n*-butane by Younglove and Ely [11].

2.2. Sample

The samples used in the experimental measurements of heat capacity were obtained from a research-grade supply. The purity of the supply has been verified by chemical analysis, establishing the purity to be 0.9999 mol fraction. The supply liquid was stored over molecular sieves to remove trace quantities of H_2O.

3. RESULTS

During the course of these measurements, pressures and temperatures were measured during each drift interval. The range of measured pressures and temperatures is depicted in the shaded area in Fig. 1. The drift interval is a 20-min period which occurs between heating intervals; it begins after thermal equilibrium has been established. In general, the temperature falls with time at a rate of about 0.5×10^{-3} K · min^{-1}, due to small parasitic heat losses, of the order of 10^{-3} W. From these pressures and temperatures, we have calculated the densities of the sample confined to the bomb under dynamic equilibrium conditions. In addition, we have devised a control scheme to hold the bomb at a fixed temperature while the equilibrium pressure is measured. We then measured one or more static points on each isochore and calculated the liquid density under static equilibrium.

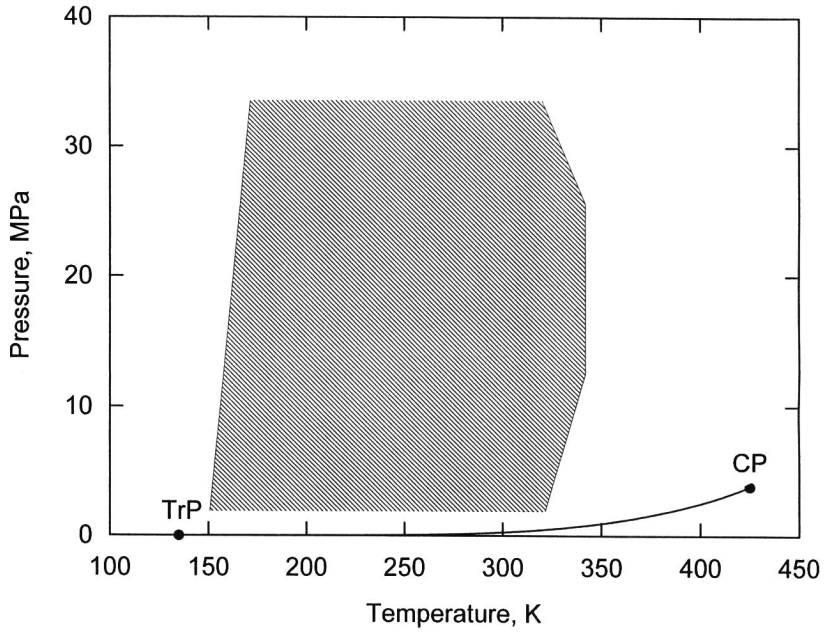

Fig. 1. Range of experimental pressures and temperatures for *n*-butane heat capacity measurements.

There are two purposes for these density tests. The first purpose is to determine the difference between the density obtained under dynamic and that obtained under static equilibrium conditions. The second purpose is to compare these densities to accurate published densities. In Fig. 2, we show how densities from this work and those measured by Haynes [12] and Olds et al. [13] deviate from an equation of state published by Younglove and Ely [11]. This equation of state was developed with the data in Refs. 12 and 13 but not with the present results. The error bars in Fig. 2 signify the 0.1% uncertainty which Haynes estimates for his densities. The data from this study are shown at seven densities. The filled symbols signify static equilibrium measurements, while the open symbols of the same shape are for the dynamic points of the same isochore. Figure 2 shows that the static and dynamic densities on a given isochore differ by less than 0.02%, with the static densities having the larger values. This supports our claim that, since the parasitic heat losses are small, the pressures and temperatures during the drift measurements are reliable enough to extract useful densities which have only slightly higher uncertainties than the static equilibrium measurements. We also note that there is a small systematic

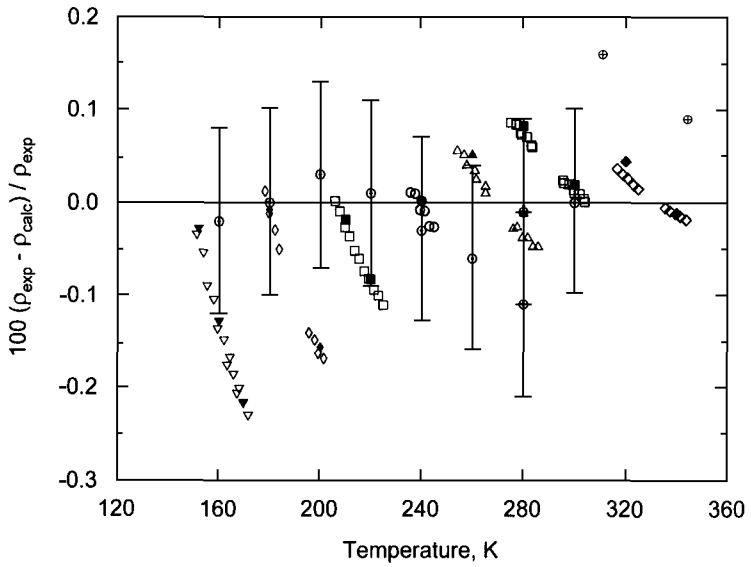

Fig. 2. Comparison of experimental density results for *n*-butane with the values calculated with the equation of state of Ref. 11. Open symbols, dynamic; filled symbols, static. (⊙) Haynes [12]; (⊕) Olds et al. [13].

difference between the densities from the calorimeter and those calculated with the equation in Ref. 11. The trend shows that the calculated densities become larger than the experimental densities by up to 0.23% as the pressure increases to about 35 MPa. Nevertheless, all of these deviations fall within the combined uncertainty of the present densities and those used to develop the equation of state in Ref. 11. The second result is that all of the densities obtained under dynamic equilibrium are within 0.2% of the Haynes [12] data and the Olds et al. [13] data. This result supports our earlier determination, based on propagation of uncertainties, that the densities from this experiment have an uncertainty of 0.2%.

The heat-capacity data are presented in Table I for two-phase states and in Table II for single-phase liquid states. The average temperature of the heating interval is given under the temperature headings. In the two-phase region, most of the measured vapor pressures are below the range of high-accuracy readings of the pressure gauge (3–70 MPa). Thus the pressures, which were required for corrections, were calculated from a vapor-pressure equation [11] but are not presented in Table I. In the single-phase liquid region, the pressures are calculated from pseudo-isochoric fits of the (p, T) data of each isochore. A seven-term equation obtained from the equation of state of Jacobsen and Stewart [14] is used

Table I. Measurements of Heat Capacity C_σ for Saturated Liquid *n*-Butane[a]

T_a (K)	ρ_a (mol·dm^{-3})	$C_v^{(2)}$ (J·mol^{-1}·K^{-1})	C_σ (J·mol^{-1}·K^{-1})
141.736	12.420	114.64	114.64
145.858	12.419	114.78	114.78
140.506	11.239	114.86	114.86
144.361	11.237	114.87	114.87
148.185	11.235	115.13	115.13
151.978	11.234	115.28	115.28
155.744	11.232	115.61	115.61
159.480	11.231	115.86	115.86
163.186	11.229	115.99	115.99
166.868	11.227	116.30	116.30
170.524	11.226	116.42	116.42
174.155	11.224	116.49	116.49
177.758	11.222	117.12	117.12
181.345	11.221	117.48	117.48
184.906	11.219	117.69	117.69
188.441	11.218	117.91	117.91
191.953	11.216	118.46	118.45
195.449	11.214	119.11	119.11
198.917	11.213	119.18	119.17
202.365	11.211	119.95	119.95
205.793	11.210	120.08	120.08
209.196	11.208	120.78	120.78
215.951	11.205	121.74	121.74
219.297	11.203	122.34	122.35
138.610	9.512	114.63	114.63
143.488	9.510	114.80	114.80
148.312	9.509	115.22	115.22
153.088	9.507	115.28	115.28
157.818	9.505	115.51	115.51
162.481	9.504	115.81	115.80
167.077	9.502	116.26	116.26
171.653	9.500	116.48	116.47
176.188	9.498	116.97	116.96
180.686	9.497	117.38	117.37
185.152	9.495	117.70	117.68
189.565	9.493	117.99	117.97
193.941	9.492	118.44	118.42
198.281	9.490	119.36	119.33
202.613	9.488	119.61	119.57
211.142	9.485	120.87	120.81

[a] T_a, temperature (ITS-90); ρ_a, bulk density; and $C_v^{(2)}$, two-phase heat capacity. The subscript *a* denotes a condition evaluated at the average of the initial and final temperatures.

Table I. (*Continued*)

T_a (K)	ρ_a (mol · dm^{-3})	$C_v^{(2)}$ (J · mol^{-1} · K^{-1})	C_σ (J · mol^{-1} · K^{-1})
215.355	9.483	121.47	121.40
219.550	9.481	122.27	122.20
223.729	9.480	123.17	123.08
227.884	9.478	123.84	123.74
232.009	9.476	124.18	124.07
236.102	9.475	125.01	124.89
240.170	9.473	126.16	126.03
244.213	9.471	126.69	126.56
248.231	9.470	127.58	127.43
252.227	9.468	128.41	128.27
256.177	9.466	129.24	129.10
260.092	9.465	130.31	130.17
263.986	9.463	131.25	131.12
267.856	9.461	132.16	132.04
271.707	9.460	133.20	133.09
275.540	9.458	134.20	134.11
279.353	9.456	135.10	135.04
283.147	9.455	136.09	136.08
286.927	9.453	137.30	137.33
298.207	9.448	140.05	140.29
301.952	9.447	141.44	141.77
305.675	9.445	142.41	142.85
309.400	9.443	143.73	144.29
313.072	9.442	145.03	145.72
316.748	9.440	145.70	146.55
142.674	9.913	114.69	114.69
147.362	9.911	114.92	114.92
152.009	9.910	115.36	115.35
156.619	9.908	115.67	115.67
161.179	9.906	115.98	115.98
165.703	9.905	116.03	116.03
170.185	9.903	116.20	116.20
174.627	9.901	116.59	116.59
179.035	9.899	117.20	117.20
183.410	9.898	117.29	117.28
187.738	9.896	117.82	117.80
192.026	9.894	118.67	118.65
196.288	9.892	119.22	119.19
200.506	9.891	119.56	119.53
204.697	9.889	120.22	120.19
208.880	9.887	120.71	120.67
213.012	9.885	121.28	121.23
217.117	9.884	121.87	121.82
221.204	9.882	122.29	122.24

Table I. (*Continued*)

T_a (K)	ρ_a (mol·dm^{-3})	$C_v^{(2)}$ (J·mol^{-1}·K^{-1})	C_σ (J·mol^{-1}·K^{-1})
276.460	9.858	134.29	134.37
280.673	9.856	135.46	135.58
284.858	9.854	136.46	136.64
289.029	9.852	137.19	137.45
293.163	9.850	138.37	138.71
225.258	9.880	123.10	123.03
229.288	9.879	124.07	124.00
233.281	9.877	124.81	124.74
241.193	9.873	126.41	126.33
245.104	9.872	127.03	126.95
249.002	9.870	127.56	127.48
256.729	9.867	129.30	129.24
260.558	9.865	130.61	130.57
264.358	9.863	131.31	131.28
268.135	9.862	132.39	132.39
271.899	9.860	132.87	132.90

Table II. Measurements of Heat Capacity C_v for Liquid *n*-Butane[a]

T_a (K)	ρ_a (mol·dm^{-3})	p (MPa)	C_v (J·mol^{-1}·K^{-1})
153.289	12.392	5.317	84.47
155.898	12.384	9.548	84.23
157.373	12.379	11.931	85.04
159.944	12.371	16.042	84.72
161.407	12.367	18.355	85.51
163.954	12.359	22.330	85.42
165.406	12.355	24.568	85.65
166.370	12.352	26.046	85.37
167.931	12.347	28.426	85.77
170.046	12.340	31.633	85.76
164.977	12.200	4.216	84.48
167.251	12.194	7.632	84.45
169.003	12.188	10.264	84.79
171.267	12.182	13.650	84.89
173.000	12.177	16.219	85.27
175.248	12.170	19.514	85.34

[a] T_a, temperature (ITS-90); ρ_a, density; and p, pressure. The subscript *a* denotes a condition evaluated at the average of the initial and final temperatures.

Table II. (*Continued*)

T_a (K)	ρ_a (mol·dm^{-3})	p (MPa)	C_v (J·mol^{-1}·K^{-1})
176.963	12.165	21.998	85.70
179.192	12.159	25.187	85.76
180.887	12.154	27.584	86.11
183.101	12.147	30.689	86.19
180.179	11.969	5.214	85.00
181.823	11.965	7.504	84.89
184.147	11.958	10.705	85.07
185.779	11.954	12.931	85.30
188.082	11.948	16.050	85.73
189.695	11.943	18.219	85.94
191.993	11.937	21.288	85.75
193.583	11.933	23.396	86.52
195.858	11.926	26.386	86.35
197.440	11.922	28.444	86.86
199.703	11.916	31.354	87.19
203.898	11.588	4.688	86.20
205.777	11.584	6.945	86.33
207.788	11.579	9.348	86.70
209.640	11.574	11.546	86.88
211.646	11.569	13.911	86.85
213.476	11.565	16.054	87.59
215.470	11.560	18.373	87.46
217.283	11.555	20.466	88.12
219.269	11.551	22.740	88.67
221.059	11.546	24.775	88.52
223.040	11.541	27.012	88.82
224.801	11.537	28.983	89.39
226.766	11.532	31.168	89.57
228.011	11.179	3.113	88.23
229.922	11.175	5.087	88.66
231.823	11.171	7.039	88.96
233.723	11.167	8.980	89.32
235.610	11.163	10.897	89.69
237.494	11.159	12.800	90.05
239.367	11.155	14.680	90.38
241.237	11.150	16.547	90.86
243.094	11.146	18.389	91.18
244.951	11.142	20.220	91.58
246.799	11.138	22.031	91.95
248.643	11.134	23.827	92.23
250.484	11.130	25.608	92.63
252.302	11.127	27.356	93.17
254.140	11.123	29.111	93.20
255.945	11.119	30.823	94.05

Table II. (*Continued*)

T_a (K)	ρ_a (mol·dm^{-3})	p (MPa)	C_v (J·mol^{-1}·K^{-1})
257.767	11.115	32.539	94.59
254.576	10.735	3.343	91.82
255.941	10.732	4.537	92.03
258.829	10.727	7.051	92.63
259.640	10.725	7.754	92.76
263.048	10.719	10.691	93.30
263.325	10.718	10.928	93.51
266.979	10.711	14.044	94.26
267.239	10.711	14.265	94.41
270.622	10.704	17.119	95.19
271.406	10.703	17.777	95.59
274.236	10.697	20.139	96.00
275.542	10.695	21.223	96.33
277.829	10.691	23.112	96.56
279.648	10.687	24.606	97.18
281.664	10.683	26.254	97.65
283.724	10.680	27.926	97.85
285.734	10.676	29.550	98.74
287.775	10.672	31.187	98.62
289.777	10.668	32.782	99.51
277.132	10.326	2.725	95.80
279.246	10.322	4.304	96.54
280.953	10.319	5.576	96.63
281.336	10.319	5.860	96.64
283.445	10.315	7.424	97.18
285.142	10.312	8.677	97.48
285.511	10.312	8.949	97.67
287.619	10.308	10.499	98.37
289.304	10.305	11.733	98.29
289.659	10.305	11.993	98.57
291.768	10.301	13.530	99.07
293.439	10.299	14.742	99.56
293.783	10.298	14.991	99.69
295.888	10.294	16.511	100.11
297.551	10.292	17.706	100.32
297.882	10.291	17.943	100.52
299.988	10.288	19.449	100.88
301.642	10.285	20.626	101.13
301.959	10.284	20.851	101.44
304.057	10.281	22.337	101.76
305.707	10.278	23.499	101.99
306.011	10.278	23.713	102.47
308.110	10.274	25.184	102.88
310.042	10.271	26.532	103.39

Table II. (*Continued*)

T_a (K)	ρ_a (mol·dm^{-3})	p (MPa)	C_v (J·mol^{-1}·K^{-1})
312.138	10.267	27.987	103.24
314.052	10.264	29.310	104.14
316.141	10.261	30.747	104.45
318.047	10.258	32.053	104.67
320.133	10.254	33.476	105.82
302.143	9.830	1.903	100.78
304.202	9.827	3.178	101.00
306.326	9.824	4.489	101.72
308.426	9.820	5.781	101.89
310.496	9.818	7.051	102.86
312.632	9.814	8.357	102.94
314.644	9.812	9.583	103.60
316.825	9.808	10.908	103.58
318.784	9.806	12.093	103.82
320.996	9.803	13.427	104.88
322.900	9.800	14.570	105.19
325.153	9.797	15.919	105.60
327.010	9.794	17.026	106.16
329.288	9.791	18.380	106.86
331.112	9.788	19.459	107.30
333.419	9.785	20.820	107.63
335.207	9.782	21.869	107.92
337.527	9.779	23.226	108.05
339.283	9.776	24.249	109.35
341.620	9.773	25.606	109.37
322.540	9.421	2.228	105.03
324.767	9.418	3.402	105.42
324.940	9.418	3.493	105.29
325.884	9.416	3.990	105.87
326.758	9.415	4.450	106.21
328.987	9.412	5.620	106.31
329.229	9.412	5.747	105.98
330.156	9.411	6.233	106.00
330.964	9.410	6.655	106.84
333.208	9.407	7.828	107.22
333.499	9.407	7.980	107.40
334.401	9.406	8.450	107.27
335.153	9.405	8.842	107.06
337.424	9.402	10.023	107.59
337.770	9.401	10.202	108.15
338.649	9.400	10.658	108.46
339.331	9.399	11.012	108.42
341.611	9.397	12.192	108.23
342.004	9.396	12.395	109.35

to fit the (p, T) data of each isochore within the uncertainty of the measurements. The density, given in Table II for single-phase liquid states, is calculated from the number of moles and the bomb volume. A detailed discussion of the uncertainties of measured quantities is available in a previous work [15]. We have determined that the expanded uncertainty (i.e., a coverage factor $k = 2$ and thus a two-standard deviation estimate) of C_v is 0.7%, for $C_v^{(2)}$ it is 0.5%, and for C_σ it is 0.7%.

In Table I, values of the two-phase heat capacity at constant volume [$C_v^{(2)}$] are presented, as well as the saturated liquid heat capacity C_σ [also known as $C'_x = T(dS'/dT)$]. Values of C_σ are obtained by adjusting the $C_v^{(2)}$ data with the equation given by Rowlinson [16],

$$C_\sigma = C_v^{(2)} - \frac{T}{\rho^2}\frac{d\rho_\sigma}{dT}\frac{dp_\sigma}{dT} + T\left(\frac{1}{\rho_\sigma} - \frac{1}{\rho}\right)\frac{d^2 p_\sigma}{dT^2} \tag{3}$$

where ρ_σ and p_σ are the density and the pressure of the saturated liquid and ρ is the bulk density of the sample residing in the bomb. The derivative quantities were calculated with the ancillary equations of Younglove and Ely [11].

The saturated liquid heat capacity C_σ, as a saturation quantity, depends on a single variable—temperature. If the data are internally consistent, then the values from different isochores must fall on a single curve. Though the C_σ values were evaluated from experiments with different amounts of sample in the calorimeter, the results should demonstrate consistency of all isochores. The saturated-liquid heat capacities for all of the filling densities are depicted graphically in Fig. 3. To intercompare the data sets from different isochores, we fitted an equation to the C_σ data. This equation accurately describes the whole data set at temperatures from 139 to 317 K.

For *n*-butane, the three-parameter expression,

$$(C_\sigma/C_0) = a_1 T_r^{1/4} + a_2 T_r^{1/2} + a_3 T_r^{9/4} \tag{4}$$

where $C_0 = 1\ \mathrm{J \cdot mol^{-1} \cdot K^{-1}}$, $T_r = T/T_c$, $T_c = 425.16$ K, $a_1 = 3.8251447 \times 10^2$, $a_2 = -3.2492719 \times 10^2$, and $a_3 = 1.3907469 \times 10^2$, was fit by applying software based on the Wagner method of structural optimization [17]. The deviations of the present results and the published C_p data of Aston and Messerly [18], Dana et al. [19], and Huffman et al. [20] from Eq. (4) are shown in Fig. 4. Only the present results were used to obtain the fit. Deviations of our results are distributed randomly over the entire temperature range, with a standard deviation of the fit of 0.13%, indicating that there is a good internal consistency. The data of Aston and Messerly have

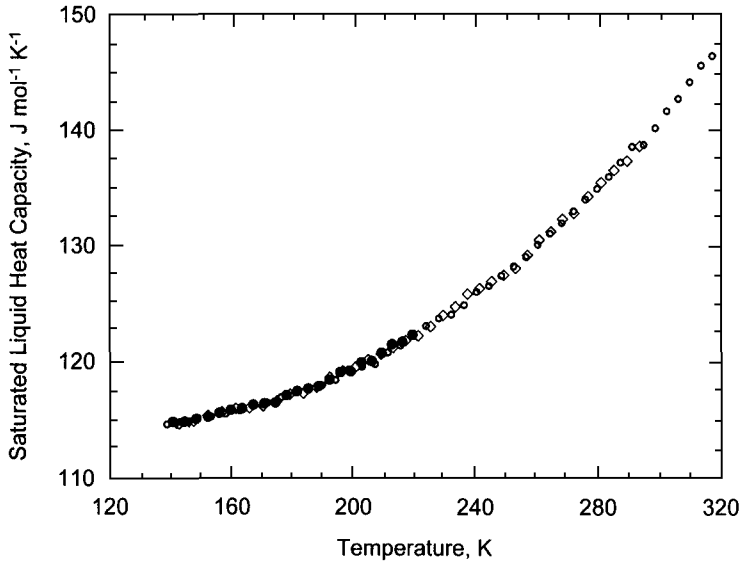

Fig. 3. Experimental saturated liquid heat-capacity (C_σ) values for *n*-butane: symbols signify different filling masses.

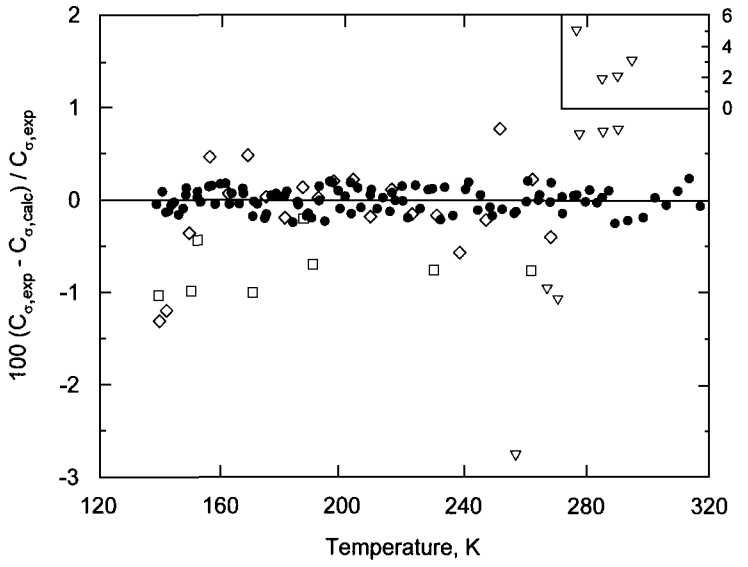

Fig. 4. Comparison of experimental C_σ results for *n*-butane with the values calculated with Eq. (4). (●) this work; (◇) Aston and Messerly [18]; (▽) Dana et al. [19]; (□) Huffman et al. [20].

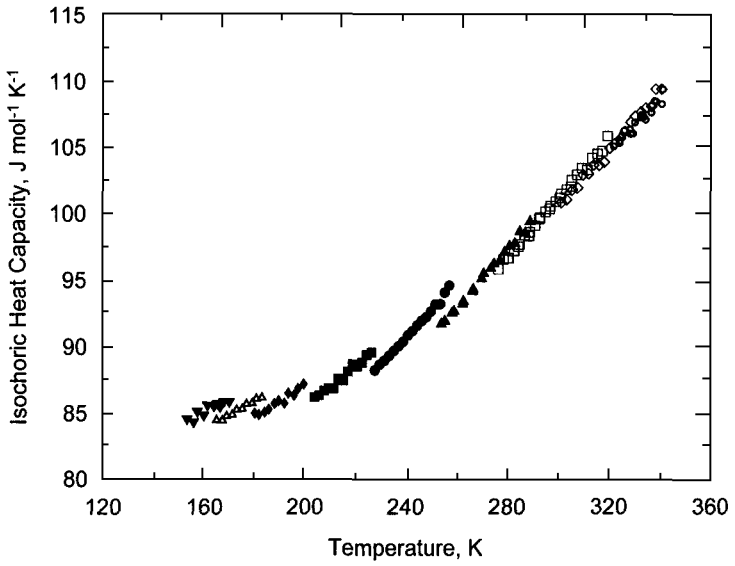

Fig. 5. Experimental liquid-phase heat-capacity (C_v) data for *n*-butane.

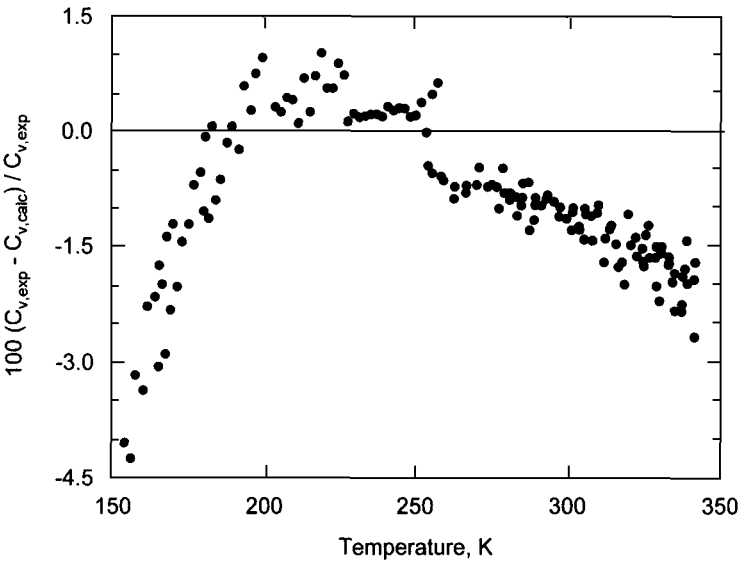

Fig. 6. Comparison of experimental C_v data for *n*-butane from this work with the values calculated using an equation of state [11].

a claimed uncertainty of 0.5% and show excellent agreement with our results. The data of Huffman et al. have an uncertainty of 1% and agree with our results to within this claim. The data of Dana et al. have a claimed uncertainty of 2% but show discrepancies from Eq. (4) of as much as 5%. However, a closer examination of the C_p data of Dana et al. reveals a scatter of approximately 7% in their measurements, which leads us to conclude that the uncertainty of their data cannot be less than this quantity.

Values of the single-phase liquid heat capacity are shown in Fig. 5. The data are presented on isochores in a C_v–T diagram. Most isochores overlap in their temperature ranges. Figure 5 shows that for *n*-butane, the slope of each C_v–T isochore is nearly independent of the density of the isochore. Thus, almost all of the *n*-butane data fall on a simple curve.

Often, when equations of state based solely on (p, ρ, T) data are used for predicting heat capacities of liquids, they give predictions that have considerable uncertainty. Since the equation of state of Younglove and Ely [11] is one of the most accurate models available for *n*-butane, we decided to test it with the measured values of this study. Younglove and Ely estimated that calculated heat capacities have an uncertainty of $\pm 2\%$ at temperatures below T_c in the liquid phase. Figure 6 shows the results of this comparison. The calculated C_v values used for Fig. 6 were derived from this equation of state using the relation,

$$C_v(T, \rho) = C_v^0(T) - T \int_0^\rho (\partial^2 p/\partial T^2)_\rho \, d\rho/\rho^2 \tag{5}$$

where C_v^0 is the heat capacity for the ideal gas. Figure 6 shows that most of the predicted values are within $\pm 2\%$ of the measurements, except for those at temperatures below 180 and above 320 K. There are strong systematic deviations between the data and the predicted heat capacities. Most of the predicted values are larger than our experimental results. Overall, the root-mean-square deviation of the experimental C_v results from the calculated values is 1.38%, which is good agreement. However, if experimental C_v data had been available when Younglove and Ely optimized their equation of state, this agreement would have been much better.

4. CONCLUSIONS

For *n*-butane, we have reported 148 C_v and 100 C_σ values. Examination of both dynamically and statically measured liquid densities from this study shows that the agreement with published data is within 0.2%. Agreement was within 1% for reliable published heat capacities at constant

pressure C_p for the saturated liquid. No published liquid C_v data were found for comparison. Comparisons with C_v values calculated with a published equation of state show that sytematic deviations exist which are larger than our claimed uncertainty. We recommend the formulation of a new equation of state for *n*-butane which incorporates recently published experimental data.

ACKNOWLEDGMENTS

We are grateful to Ben Younglove and Marcia Huber for generous technical assistance and helpful discussions during this study. We acknowledge the Ernest-Solvay Foundation for the financial support of Torsten Lüddecke during his guest researcher appointment at the NIST. We have profited from many discussions with Tom Bruno, Dan Friend, W. M. Haynes, Arno Laesecke, and Lloyd Weber.

REFERENCES

1. B. A. Younglove, *J. Res. Natl. Bur. Stand. (U.S.)* **78A**:401 (1974).
2. H. M. Roder, *J. Res. Natl. Bur. Stand. (U.S.)* **80A**:739 (1976).
3. R. D. Goodwin, *J. Res. Natl. Bur. Stand. (U.S.)* **83**:449 (1978).
4. J. E. Mayrath and J. W. Magee, *J. Chem. Themodyn.* **21**:499 (1989).
5. J. W. Magee, *J. Chem. Eng. Data* **40**:438 (1995).
6. W. M. Haynes and R. D. Goodwin, *Thermophysical Properties of Normal Butane from 135 to 700 K at Pressures to 70 MPa*, National Bureau of Standards (U.S.) Monograph 169, (U.S. GPO, Washington, DC, 1982).
7. V. V. Sychev, A. A. Vasserman, A. D. Kozlov, and V. A. Tsymarny, *Thermodynamic Properties of Butane* (Begell House, New York, 1995).
8. R. D. Goodwin, *J. Res. Natl. Bur. Stand. (U.S.)* **65C**:231 (1961).
9. J. W. Magee, *J. Res. Natl. Inst. Stand. Technol.* **96**:725 (1991).
10. R. D. Goodwin and L. A. Weber, *J. Res. Natl. Bur. Stand. (U.S.)* **73A**:1 (1969).
11. B. A. Younglove and J. F. Ely, *J. Phys. Chem. Ref. Data* **16**:577 (1987).
12. W. M. Haynes, *J. Chem. Themodyn.* **15**:801 (1983).
13. R. H. Olds, H. H. Reamer, B. H. Sage, and W. N. Lacey, *Ind. Eng. Chem.* **36**:282 (1944).
14. R. T Jacobsen and R. B. Stewart, *J. Phys. Chem. Ref. Data* **2**:757 (1973).
15. T. O. Lüddecke and J. W. Magee, *Int. J. Thermophys.* **17**:823 (1996).
16. J. S. Rowlinson, *Liquids and Liquid Mixtures* (Butterworths, London, 1969), p. 37.
17. W. Wagner, *Eine mathematisch statistische Methode zum Aufstellen thermodynamischer Gleichungen—gezeigt am Beispiel der Dampfdruckgleichung reiner Fluide*, Habilitationsschrift TU Braunschweig, FortschrBer. VDI-Z. Reihe 3, Nr. 39 (VDI, Düsseldorf, 1974).
18. J. G. Aston and G. H. Messerly, *J. Am. Chem. Soc.* **62**:1917 (1940).
19. L. I. Dana, A. C. Jenkins, J. N. Burdick, and R. C. Timm, *Refrig. Eng.* **12**:387 (1926).
20. H. M. Huffman, G. S. Parks, and M. Barmore, *J. Am. Chem. Soc.* **53**:3876 (1931).